Probing Local Hydrogen Impurities in Quasi-Free-Standing Graphene

Martha Scheffler,[†,⊥,*] Danny Haberer,[†,*] Luca Petaccia,[‡] Mani Farjam,[§] Ronny Schlegel,[†] Danny Baumann,[†] Torben Hänke,[†] Alexander Grüneis,[†,∥] Martin Knupfer,[†] Christian Hess,[†] and Bernd Büchner[†,⊥]

[†]IFW Dresden, P.O. Box 270116, D-01171 Dresden, Germany, [‡]Elettra Sincrotrone Trieste, Strada Statale 14 Km 163.5, 34149 Trieste, Italy, [§]School of Nano-Science, Institute for Research in Fundamental Sciences (IPM), P.O. Box 19395-5531, Tehran, Iran, [⊥]Institut für Festkörperphysik, TU Dresden, D-01069 Dresden, Germany, and [∥]Faculty of Physics, University of Vienna, Strudlhofgasse 4, 1090 Wien, Austria

ABSTRACT We report high-resolution scanning tunneling microscopy and spectroscopy of hydrogenated, quasi-free-standing graphene. For this material, theory has predicted the appearance of a midgap state at the Fermi level, and first angle-resolved photoemission spectroscopy (ARPES) studies have provided evidence for the existence of this state in the long-range electronic structure. However, the spatial extension of H defects, their preferential adsorption patterns on graphene, or local electronic structure are experimentally still largely unexplored. Here, we investigate the shapes and local electronic structure of H impurities that go with the aforementioned midgap state observed in ARPES. Our measurements of the local density of states at hydrogenated patches of graphene reveal a hydrogen impurity state near the Fermi level whose shape depends on the tip position with respect to the center of a patch. In the low H concentration regime, we further observe predominantly single hydrogenation sites as well as extended multiple C—H sites in parallel orientation to the lattice vectors, indicating an adsorption at the same graphene sublattice. This is corroborated by ARPES measurements showing the formation of a dispersionless hydrogen impurity state which is extended over the whole Brillouin zone.

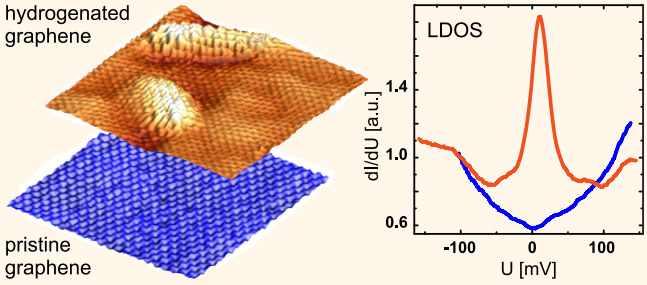

KEYWORDS: scanning tunneling microscopy · scanning tunneling spectroscopy · graphene · hydrogenation · photoemission spectroscopy

Graphene currently receives enormous attention due to its peculiar electronic and mechanical properties.[1−3] Especially by tailoring its electronic properties employing chemical functionalization, graphene provides an enormous application potential regarding electronic devices,[4,5] sensors,[6,7] or spintronics.[8,9] Hence, understanding the influence of impurities on the local electronic properties of graphene is crucial from a fundamental as well as application-oriented point of view. Model calculations[10,11] as well as microscopic investigations[12,13] of different adatoms on graphene have shown that functionalization by impurities induces disorder in the system and yields localized states.[14]

However, most insulating as well as metallic substrates employed for graphene fabrication and characterization already act as dopant or strongly interact with the out-of-plane π orbitals of graphene.[15−20] In order to study the intrinsic electronic structure of functionalized graphene using local scale scanning tunneling microscopy and spectroscopy (STM/STS) as well as spatially averaging ARPES, a substrate is required that does not significantly interact with the electronic structure of graphene. It was previously shown by ARPES that intercalation of a Au monolayer between a CVD-grown single-crystalline graphene sheet and its Ni(111) substrate substantially reduces the interactions and recovers the Dirac fermion behavior.[21−23] Another approach to obtain graphene that does not significantly interact with its substrate was first demonstrated by Riedl *et al.*[24] when intercalating epitaxial graphene on SiC with hydrogen. Hence, these systems are suitable candidates for investigations of the local electronic structure with both local as well as spatially averaged spectroscopic methods.

Here we investigate the electronic properties of hydrogenated quasi-free graphene on a metal substrate on a local scale with

* Address correspondence to m.scheffler@ifw-dresden.de, danny.haberer@gmail.com.

Received for review August 2, 2012 and accepted November 18, 2012.

Published online November 18, 2012
10.1021/nn303485c

STM and STS in combination with ARPES. We show that our starting material, graphene on Au, exhibits a high crystalline quality with no observable defects or adsorbates on the local scale, which is a crucial precondition for studies of artificial impurities. We probe the topography as well as the local density of states (LDOS) with STM/STS in subnanometer resolution and find pronounced impurity states at hydrogenation sites with position-dependent shapes and widths. In contrast to measurements of graphene on Ir(111) with stronger substrate interaction, where a full hydrogenation of the graphene was shown,[25] we focus in this work on well-isolated hydrogenated sites. The comparison of shape and size of the obtained hydrogenated patches with density functional based tight binding method (DFTB) calculations suggests that atomic hydrogen adsorbs on graphene in the low concentration regime giving rise to single and extended double or triple C−H sites with spatial orientations that follow that of a meta configuration. The studies of the local electronic structure of hydrogenated graphene are corroborated by complementary ARPES measurements. We demonstrate the formation of a hydrogen impurity state across the Brillouin zone and further discuss the p-type doping induced by hydrogen impurities on graphene.

RESULTS AND DISCUSSION

Figure 1a shows a typical topographic image of as-produced graphene on a Ni(111) substrate. The inset represents the fast Fourier transform (FFT) of the image from which we determine the lattice constant within given accuracy to 2.4(±0.1) Å (consistent with the expected value for graphene of 2.46 Å). The graphene layer covers the substrate homogeneously and across step edges as it is expected from the CVD growth on single-crystalline substrates.[26−28] Furthermore, we do not observe significant lattice distortions, defects, or adsorbates neither on the local atomic scale (50 nm × 50 nm) nor on larger areas (shown in Figure S1 of the Supporting Information) which outlines the high quality of the obtained graphene. However, its electronic structure is strongly modified by the Ni substrate due to hybridization[29,30] which in turn affects the spectroscopic measurements. Figure 1b depicts a typical STS spectrum of graphene/Ni(111) obtained at 300 K. The recorded LDOS exhibits two prominent features at around −400 mV and +450 mV bias voltage, which are related to the spin-split band edges of the Ni band structure and, thus, the electronic structure of the substrate rather than that of graphene.[31,32] In order to investigate the local electronic properties of graphene, and subsequently those of hydrogen adsorbates, a liberation from the Ni substrate is crucial.

The intercalation of one monolayer (ML) Au effectively decouples graphene electronically from the Ni substrate[21−23] and induces a Moiré superstructure in

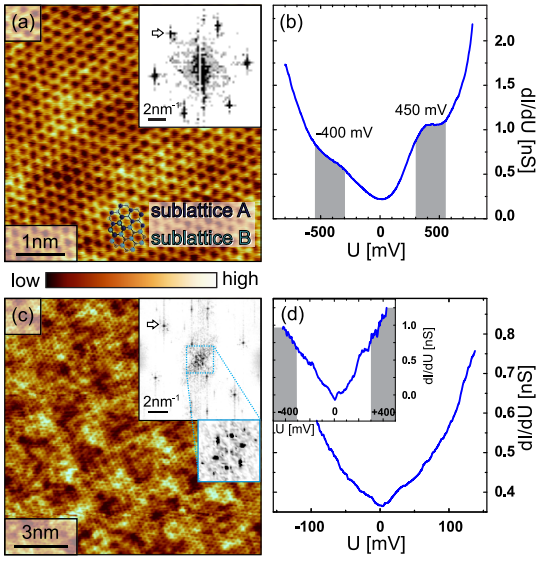

Figure 1. (a) Atomically resolved topography image of as-produced graphene on Ni(111). No significant defects on all investigated areas were observed. Inset: FFT, spots correspond to lattice constant of 2.4 Å (I = 0.8 nA, U = −250 mV). (b) dI/dU spectrum (average over 8 × 8 spectroscopic map of 5 nm ×5 nm) of graphene/Ni(111). Shoulders at around −400 mV and 400 mV refer to the Ni electronic structure and prevent an investigation of bare graphene (I = 0.25 nA, U = −600 mV, U_{mod} = 10 mV, T = 300 K). (c) Topography of graphene intercalated with 1 ML Au leading to a lattice mismatch induced Moiré pattern. Inset: FFT, outer spots correspond to a lattice constant of 2.4 Å. Inner spots depicted in the zoomed image are related to the Moiré pattern with a lattice constant of 27.4 Å (I = 0.5 nA, U = −100 mV, T = 20 K). (d) dI/dU curves of graphene after Au intercalation, averaged over a 5 × 5 spectroscopic map of 5 nm × 5 nm. The quasi-free-standing graphene exhibits a nearly linear, symmetric shape in the LDOS with a minimum at the Fermi energy (I = 0.5 nA, U = −100 mV, U_{mod} = 4 mV, T = 20 K). Inset: larger bias scale, averaged over 10 single-point spectra (I = 0.5 nA, U = −400 mV, U_{mod} = 4 mV, T = 20 K).

topography images due to a lattice mismatch between Au and graphene[22,23] (further topographic images of larger areas for graphene/Au are shown in Figure S2 of the Supporting Information). In Figure 1c, a region of the sample with the superstructure after Au intercalation is shown. The FFT in the inset indicates the hexagonal graphene lattice as well as the additional reflexes of the Moiré pattern, which relate to a gold lattice constant of 27.4 Å, in agreement with previous values.[22,23] The superstructure is also observed for larger sample areas as well as in low energy electron diffraction (see Supporting Information) and thus indicates a fully developed Au intercalation.

The electronic properties of the graphene/Ni(111) system are strongly influenced by the Au intercalation process, as it shifts the chemical potential of graphene by 2 eV and recovers the Dirac fermion behavior of charge carriers near the Fermi level.[22] The dI/dU curve in Figure 1d follows the typical V shape as expected for the graphene DOS from band structure calculations.[33,34] For graphene on top of 1 ML Au, we identify the Dirac point at the minimum of the spectrum. In our

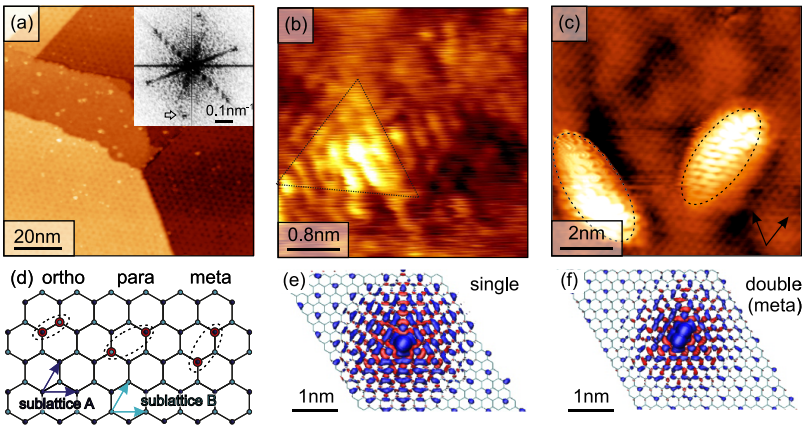

Figure 2. (a) Graphene on Au after controlled hydrogen exposure. The Moiré pattern with a corresponding lattice constant of 27 Å is also found in the FFT (inset). Bright spots are hydrogen adsorption sites (I = 0.2 nA, U = −50 mV, T = 20 K). (b,c) Atomically resolved topography images near hydrogen adsorption sites (I = 0.5 nA, U = −20 mV, T = 20 K). On the bright spots, the graphene lattice appears distorted. Dashed lines correspond to impurity shapes suggested by DFTB-based model calculations. (d) Sketch of double hydrogenation sites employed in the calculation. Calculated charge density distributions, where blue/red color shows a ± isosurface, for (e) a single C−H site and (f) a double C−H site in meta configuration describing the experimental topographies in (b) and (c), respectively.

system, we observe a slight shift of the Dirac point to positive bias voltage by about 4 mV, which is within the resolution limit. Hence, the intrinsic doping level of graphene in the investigated system is close to charge neutrality, which is in agreement with ARPES measurements[22] and similar by trend to previous works for quasi-free graphene on a graphite substrate.[35] As can be seen on the large bias scale in the inset, the features at −400 mV and +450 mV in the dI/dU curves, originating from the Ni(111) substrate, are now sufficiently reduced, especially the plateau at positive bias voltage. We also do not observe a significant variation in the dI/dU curves when comparing spectra obtained from bright and dark regions of the Moiré pattern (see Supporting Information). Hence, graphene on 1 ML Au provides a suitable base to study the local electronic properties of adsorbed impurities such as atomic hydrogen, which is presented in the following.

Figure 2a shows a large area topography scan of graphene over several terraces after hydrogenation for 10 s at 5 × 10^{-9} mbar. In addition to the honeycomb lattice, we observe randomly distributed but yet isolated bright spots, which are assigned to H impurities,[36−38] and further indicate a low concentration of adsorbates. From the large area scans, we estimate a hydrogen coverage of approximately 0.02%. The Moiré superstructure detected in the FFT (inset) is slightly diffuse due to the step edges of the substrate and the presence of H impurities which interfere with the lattice symmetry of graphene. Figure 2b,c contains atomic-resolution topography images of the hydrogenation sites, which are representative for all investigated areas on the sample. Owing to the high mobility of hydrogen impurities, the mapping of the hydrogen spots with an STM tip is only possible under particular conditions, such as low bias and slow scanning speed. With the chosen scanning parameters, we measure very close to the emerging H impurity state (see Figure 3a) and probe therefore the spatial extension of this state. The structural relaxation of the lattice leads to a strong physical as well as electronic distortion of nearby bonds, which is observed in the high-resolution STM images, where the bonding partner of the impurity in sublattice A results in a localization of the impurity state in sublattice B and at the impurity atom.[11,39] We have investigated several different hydrogenation sites on the sample and find two predominant shapes in the atomically resolved scans (additional topographies of hydrogenation sites from different regions on the sample are shown in Figure S3 of the Supporting Information). Some patches are confined and have a rather circular or sometimes a triangular form (Figure 2b), while others exhibit a more elongated shape (Figure 2c). Hence, the observed structures may correspond to the theoretically predicted appearance of single site[39] as well as double site impurities[40,41] and are furthermore similar to previously reported H monomer and (extended) dimer structures on top of graphene on SiC.[38]

In order to assign the observed topographic shapes, we have performed DFTB-based calculations of the charge density distribution for single and double H impurity sites. In Figure 2e,f, we show the expected spatial extension of a single and a double site in a meta configuration, which implies H adsorption on the same graphene sublattice as indicated in the sketch of Figure 2d. The blue parts correspond to excess electron density and are therefore comparable with a high STM intensity in the negative bias range. According to the calculation, a single hydrogen impurity introduces a (D_{3h}) symmetry of the wave function in close vicinity of the C−H site, which induces a triangular pattern in the

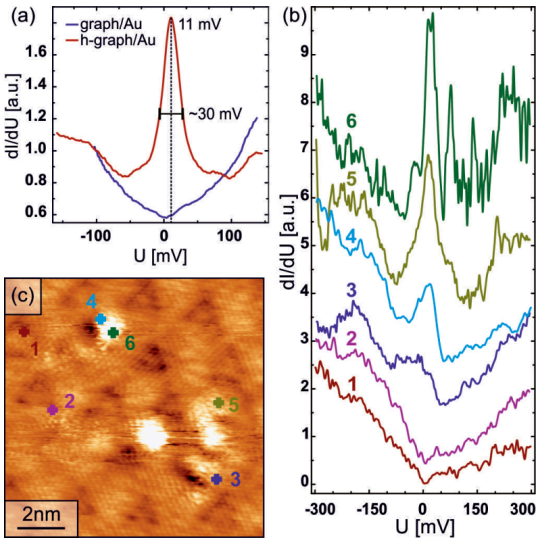

Figure 3. Tunneling spectroscopy of hydrogenated graphene. (a) Averaged d*I*/d*U* spectra of pristine graphene/Au (blue; $I = 0.5$ nA, $U = -100$ mV, $U_{mod} = 4$ mV, $T = 20$ K; 5 × 5 spectroscopic map of 5 nm × 5 nm) and hydrogenated graphene/Au (red; $I = 0.4$ nA, $U = -150$ mV, $U_{mod} = 4$ mV, $T = 20$ K; 8 × 2 single spectra on H impurities). Normalization to 1 au at −100 mV was carried out. The peak in the LDOS due to the hydrogen-induced impurity state is located at 11 ± 1 mV. (b) Single scan STS point spectra for different locations around hydrogen adsorption sites. The asymmetry of the V-shaped spectra 1 and 2 for pristine graphene is induced by the tip ((1,2,4) $I = 0.4$ nA, $U = -400$ mV, $U_{mod} = 4$ mV $T = 20$ K; (3,5,6) $I = 0.5$ nA, $U = -300$ mV, $U_{mod} = 4$ mV, $T = 20$ K). (c) Topography of hydrogen adsorption sites along with numbered spots and color code corresponding to the individual scan positions of the STS spectra in (b).

charge density distribution. It becomes nearly circular with a size of about 10 lattice constants at larger distances from the C−H bond. The spatial extension as well as the shape of the calculated charge density distribution for a single C−H site are in good agreement with the single protrusion in the STM topography, shown in Figure 2b. The elongated shapes, representatively shown in Figure 2c, point at first toward double C−H sites. In this case, three possible configurations, illustrated in Figure 2d, ortho, meta, and para which correspond to additional hydrogenation of nearest, next-nearest, and third-nearest neighbor C atoms, are conceivable. However, in our calculations, only a meta configuration as shown in Figure 2f gives rise to a spatial extension of the charge density along the zigzag edges of graphene over several lattice constants. When comparing the extension of the calculated charge density with that of the observed elongated protrusions, we find a difference in length of about three to four lattice constants. Hence, it is likely that the elongated protrusions consist of extended double or even triple hydrogenation sites oriented parallel to the lattice vectors in a meta configuration. The spacing between individual H atoms in such a configuration can be a few lattice constants, so that the high absorption barrier for a meta configuration can be reduced.[41] Nevertheless, we expect for these sites an emerging impurity state, as the orientation parallel to the lattice vectors suggests a hydrogenation of the same sublattice. This breaks, like single C−H sites, the symmetry between A and B carbon atoms and leads to the formation of a band gap as was previously shown by ARPES for higher H/C ratios and theoretical calculations.[9,23]

We now turn to the discussion of the local electronic properties in the vicinity of a hydrogenation site. The blue line in Figure 3a is a representative spectrum of the graphene LDOS acquired after annealing and before hydrogenation. The typical V shape of the spectrum indicates the electronic structure of quasi-free-standing graphene. The red d*I*/d*U* curve, averaged over 8 × 2 single-point spectra, is taken after hydrogenation at a C−H site and clearly shows an emerging H impurity state as a pronounced peak in the LDOS. At the energy of 11 ± 1 mV, the LDOS is drastically enhanced with a peak width (fwhm) of about 30 mV, in agreement with previous theoretical calculations.[39,42,43]

Similar effects in the LDOS have been observed for fluorine-doped graphene[44] as well as in graphene and graphite layers, distorted by a carbon vacancy.[45] In the work of Ugeda *et al.*,[45] it was shown that a carbon vacancy also leads to a lattice distortion and gives rise to an enhanced density of states at the Fermi energy. However, with regard to the absence of significant defects and adsorbates after the synthesis and intercalation procedure (shown in the Supporting Information), it is unlikely that the investigated triangular and elongated protrusions originate from single defects in the lattice. Furthermore, we observe that the density of bright spots is substantially increased immediately after hydrogenation and reduced to almost zero after annealing at 400−500 K, which corresponds to the desorption temperature of H.[36]

In Figure 3b, we show several single scan STS point spectra together with the topographic location of each spectrum, depicted in Figure 3c. Note that the spectra are shifted for a better presentation. All d*I*/d*U* curves obtained at or close to a hydrogenation site, as indicated in Figure 3c, exhibit an enhanced local density of states with maxima near the Fermi energy. A closer examination of the corresponding topographic sites in Figure 3c suggests that spectrum 6 is taken directly on an impurity site, which results in a rather sharp peak in the LDOS with a fwhm of about 40 mV. Spectrum 5, on the other hand, may correspond to a position of the tip over a nearest neighbor site with a less narrow and intense peak, as was calculated previously for a general defect site.[10] In comparison to the d*I*/d*U* curves 5 and 6 of Figure 3b, the peak in the spectra 3 and 4 is significantly less pronounced and much broader. It is therefore likely that these curves resemble the local electronic structure of next-nearest or more distant carbon atoms.[10,46]

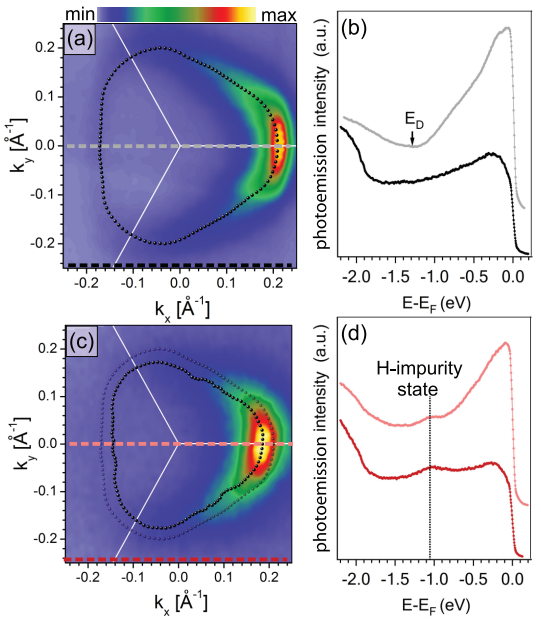

Figure 4. (a) Fermi surface map of fully K-doped graphene along with the Fermi surface contour (black dots). Dashed lines indicate cutting directions for the EDCs in (b). White solid lines mark the boundaries of the Brillouin zone. (b) EDCs along the $\Gamma-K-M$ direction (gray) and outside the Fermi surface (black). E_D indicates the position of the Dirac point. (c) Fermi surface map after hydrogenation for 10 min at 1×10^{-8} mbar. The dashed contour represents the Fermi surface of fully K-doped graphene from (a). (d) EDCs obtained from integrating along the corresponding dashed lines in (c), showing the emerging dispersionless H impurity state in the BZ.

The sharp peak in the LDOS at an impurity site provides strong evidence for a well-defined state without significant dispersion in k-space. However, with STM being a method of choice for unraveling the local electronic properties, we further employ ARPES to investigate the long-range electronic structure in k-space with high resolution. Since ARPES provides information only on the occupied states of the electronic structure, it is hardly possible to identify the impurity state located slightly above the Dirac point energy. Hence, we dope graphene with additional electrons from potassium in order to shift the Fermi level into the conduction band. The H impurity state can then be directly observed with ARPES, as we have shown previously.[46]

In Figure 4a, a 2D photoemission intensity map at E_F of fully potassium-doped graphene is shown. The Fermi surface contour, obtained from photoemission intensity maxima, exhibits a typical trigonally warped shape similar to KC_8.[47] From the enclosed k-space area, we obtain a doping of 0.061(3) extra electrons per graphene unit cell which corresponds to a shift of the Dirac point with respect to E_F of about 1.3 eV (for ARPES spectra along $\Gamma-K-M$ direction, see Supporting Information), in agreement with previous results for KC_8[47] and graphene on Ir(111).[48] In Figure 4b, we depict the integrated photoemission intensity as a function of the binding energy. The corresponding segments in the 2D Brillouin zone along which the integration is carried out are indicated in Figure 4a. The rather flat and featureless curve, obtained from a region beyond the π^* cone, is related to the electronic structure of the Au monolayer below graphene. In contrast, the cut through the K-point exhibits an increased spectral weight near E_F originating from the occupied π^*-band.

After exposing K-doped graphene to atomic hydrogen, we observe a reduction of the Fermi surface area, shown in Figure 4c, which is equivalent to a doping of 0.045(2) extra electrons per unit cell. This implies hole doping induced by the bonding hydrogen, in agreement with previous results.[46,49] Assuming one hole per attached H atom,[49] we obtain an average hydrogen concentration of $0.8 \pm 0.2\%$, which corresponds to the critical concentration for the formation of a hydrogen-derived impurity state in the long-range electronic properties.[46] Cutting the Fermi surface map at the same positions as in Figure 4a, we obtain the EDCs for hydrogenated graphene, shown in Figure 4d. Both curves clearly illustrate the manifestation of the H impurity state in the vicinity of the Dirac point. For both cuts, within and outside the π^* cone, the hydrogen-related feature is found at the same energy, which suggests, in agreement with our previous results,[46] the absence of any dispersion and extension of this state across the Brillouin zone. The impurity state observed in ARPES has a width of ~280 meV (fwhm) and is substantially broader than in the local STS spectra, which is probably attributed to the spatial insensitivity of ARPES. Hence, we observe all contributions from neighboring as well as double C–H sites[10,11] in the spectra.

CONCLUSIONS

We have demonstrated by STM/STS that *in situ* synthesized graphene/Au/Ni(111) is sufficiently well decoupled from the underlying Ni to serve as starting substrate for investigations of chemical functionalization. Furthermore, the system is, with its locally low intrinsic graphene intrinsic doping level close to neutrality, comparable with graphene on graphite[35] and thus a perfect basis to investigate the electronic properties of impurities on an atomic scale. By controlled hydrogenation, we have shown, with both local STS as well as ARPES measurements, the emergence of a hydrogen impurity state in close vicinity to the Dirac point and the propagation of the state over the whole Brillouin zone. Local measurements of the topography of the hydrogen adsorption sites have shown characteristic patterns, which have been related to simulations of single and double impurities on graphene. For the observed elongated structures, we have suggested the presence of extended double or triple C–H sites which are oriented in a meta configuration, indicating a hydrogenation of the same sublattice. The spectra we

have obtained on a local impurity site support the theoretical model for the bonding of the H adatom to the graphene lattice and the induced change of the electronic properties on nearby lattice sites.[11,39] In a future work, spin-polarized STS on these samples is suggested in order to experimentally prove the theoretically predicted spin-splitting.[42] Also for vacancies in graphene, magnetic changes in the LDOS are expected.[14,50] Our results based on graphene/Au provide a suitable basis for further studies of local magnetic moments and spin-resolved studies at impurity or defect sites.

EXPERIMENTAL METHODS

We prepared pristine monolayer graphene samples *in situ* under ultrahigh vacuum conditions by chemical vapor deposition on Ni(111) thin films, epitaxially grown on W(110).[51] Hereafter, one monolayer (ML) of Au was deposited on graphene followed by intercalation into the graphene/Ni interface by annealing at 500−600 °C.[21−23] Hydrogenation of graphene was performed at room temperature by exposing the sample to a beam of atomic H that was produced by cracking H_2 at 2800 K in a W capillary using a pressure of 5×10^{-9} mbar for 10−20 s. In order to prevent a full loss of hydrogen monomers at room temperature,[52] the sample was transferred immediately after hydrogen exposure to the STM chamber. Further details on sample preparation and hydrogenation are given in previous works.[23,53]

We used a home-built variable-temperature STM for investigation of the samples. The temperatures during STM measurements were 300 K for graphene/Ni(111) or 20 K for graphene/Au, and the pressure in the UHV preparation chamber was better than 2×10^{-9} mbar, whereas during data acquisition at 20 K, the base pressure in the STM chamber was $\leq 4 \times 10^{-10}$ mbar. The imaging of graphene was done over a wide bias range in positive and negative voltages, but most of the images shown here were taken at similar parameters of $I = (0.2...0.5)$ nA and $U = -(40...500)$ mV. Calibration of the STS spectra, shown in this work, was achieved by scanning a Au(111) thin film on mica prior to and after measuring graphene. Processing of the topographic images was carried out with the WSxM software.[54] ARPES measurements were performed at the BaDElPh beamline of the Elettra synchrotron facility in Trieste (Italy).[55] The spectra were acquired at photon energies of 29 eV with the sample at 50 K and a base pressure better than 8×10^{-11} mbar. The angular and energy resolution were set to 0.15° and 15 meV, respectively. Doping of graphene was achieved *in situ* by K evaporation from commercial SAES getters followed by thermal annealing to establish a KC_8 stoichiometry.[46] Hydrogenation was carried out with the same H source employed for functionalization in the STM setup but at a pressure of 1×10^{-8} mbar for 10 min, while the sample was kept at 50 K.

Calculations of the charge density were carried out with the density functional based tight binding (and more) ($DFTB^+$) simulation package[56,57] and the visualization by VMD.[58] A unit cell of 450 carbon atoms was applied and the difference in the two charge densities of a pristine and hydrogenated graphene lattice simulated. Blue color in the simulated images shows a positive isosurface and therefore the excess electron density, which is approximately comparable with a high STM intensity in the negative bias range.

Conflict of Interest: The authors declare no competing financial interest.

Acknowledgment. This work has been funded by the DFG through the Research Unit FOR 1154 (Grant No. HA6037/1) and the Graduate School GRK 1621. D.H., A.G., and M.K. acknowledge DFG Grant No. GR 3708/1-1. A.G. acknowledges an APART fellowship from the Austrian Academy of Sciences. D.H. and A.G. acknowledge funding from the European Community's Seventh Framework Program (FP7/2007-2013) under grant agreement 226716 for their stay at the Elettra synchrotron. D.H., L.P., and A. G. thank D. Lonza for technical assistance during the ARPES measurements. D.H. and M.S. thank R. Schönfelder, R. Hübel, S. Leger, and F. Herold for technical support. VMD was developed by the Theoretical and Computational Biophysics Group in the Beckman Institute for Advanced Science and Technology at the University of Illinois at Urbana—Champaign.

Supporting Information Available: Additional experimental details and figures. This material is available free of charge *via* the Internet at http://pubs.acs.org.

REFERENCES AND NOTES

1. Novoselov, K. S.; Geim, A. K.; Morozov, S. V.; Jiang, D.; Zhang, Y.; Dubonos, S. V.; Grigorieva, I. V.; Firsov, A. A. Electric Field Effect in Atomically Thin Carbon Films. *Science* **2004**, *306*, 666–669.
2. Geim, A. K.; Novoselov, K. S. The Rise of Graphene. *Nat. Mater.* **2007**, *6*, 183–191.
3. Geim, A. K. Graphene: Status and Prospects. *Science* **2009**, *324*, 1530–1534.
4. Sofo, J. O.; Chaudhari, A. S.; Barber, G. D. Graphane: A Two-Dimensional Hydrocarbon. *Phys. Rev. B* **2007**, *75*, 153401.
5. Elias, D. C.; Nair, R. R.; Mohiuddin, T. M. G.; Morozov, S. V.; Blake, P.; Halsall, M. P.; Ferrari, A. C.; Boukhvalov, D. W.; Katsnelson, M. I.; Geim, A. K.; *et al.* Control of Graphene's Properties by Reversible Hydrogenation: Evidence for Graphane. *Science* **2009**, *323*, 610–613.
6. Schedin, F.; Geim, A. K.; Morozov, S. V.; Hill, E. W.; Blake, P.; Katsnelson, M. I.; Novoselov, K. S. Detection of Individual Gas Molecules Adsorbed on Graphene. *Nat. Mater.* **2007**, *6*, 652–655.
7. Dan, Y.; Lu, Y.; Kybert, N. J.; Luo, Z.; Johnson, A. T. C. Intrinsic Response of Graphene Vapor Sensors. *Nano Lett.* **2009**, *9*, 1472–1475.
8. Yazyev, O. V.; Helm, L. Defect-Induced Magnetism in Graphene. *Phys. Rev. B* **2007**, *75*, 125408.
9. Boukhvalov, D. W.; Katsnelson, M. I.; Lichtenstein, A. I. Hydrogen on Graphene: Electronic Structure, Total Energy, Structural Distortions and Magnetism from First-Principles Calculations. *Phys. Rev. B* **2008**, *77*, 035427.
10. Wehling, T. O.; Balatsky, A. V.; Katsnelson, M. I.; Lichtenstein, A. I.; Scharnberg, K.; Wiesendanger, R. Local Electronic Signatures of Impurity States in Graphene. *Phys. Rev. B* **2007**, *75*, 125425.
11. Wehling, T. O.; Katsnelson, M. I.; Lichtenstein, A. I. Impurities on Graphene: Midgap States and Migration Barriers. *Phys. Rev. B* **2009**, *80*, 085428.
12. Brar, V. W.; Decker, R.; Solowan, H.-M.; Wang, Y.; Maserati, L.; Chan, K. T.; Lee, H.; Girit, C. O.; Zettl, A.; Louie, S. G.; *et al.* Gate-Controlled Ionization and Screening of Cobalt Adatoms on a Graphene Surface. *Nat. Phys.* **2011**, *7*, 43–47.
13. Gyamfi, M.; Eelbo, T.; Waśniowska, M.; Wiesendanger, R. Fe Adatoms on Graphene/Ru(0001): Adsorption Site and Local Electronic Properties. *Phys. Rev. B* **2011**, *84*, 113403.
14. Pereira, V. M.; Guinea, F.; Lopes dos Santos, J. M. B.; Peres, N. M. R.; Castro Neto, A. H. Disorder Induced Localized States in Graphene. *Phys. Rev. Lett.* **2006**, *96*, 036801.
15. Dedkov, Y. S.; Shikin, A. M.; Adamchuk, V. K.; Molodtsov, S. L.; Laubschat, C.; Bauer, A.; Kaindl, G. Intercalation of Copper Underneath a Monolayer of Graphite on Ni(111). *Phys. Rev. B* **2001**, *64*, 035405.
16. Giovannetti, G.; Khomyakov, P. A.; Brocks, G.; Kelly, P. J.; van den Brink, J. Substrate-Induced Band Gap in Graphene on Hexagonal Boron Nitride: *Ab Initio* Density Functional Calculations. *Phys. Rev. B* **2007**, *76*, 073103.

17. Marchini, S.; Günther, S.; Wintterlin, J. Scanning Tunneling Microscopy of Graphene on Ru(0001). *Phys. Rev. B* **2007**, *76*, 075429.
18. Uchoa, B.; Lin, C.-Y.; Castro Neto, A. H. Tailoring Graphene with Metals on Top. *Phys. Rev. B* **2008**, *77*, 035420.
19. Geringer, V.; Liebmann, M.; Echtermeyer, T.; Runte, S.; Schmidt, M.; Rückamp, R.; Lemme, M. C.; Morgenstern, M. Intrinsic and Extrinsic Corrugation of Monolayer Graphene Deposited on SiO_2. *Phys. Rev. Lett.* **2009**, *102*, 076102.
20. Pletikosic, I.; Kralj, M.; Pervan, P.; Brako, R.; Coraux, J.; N'Diaye, A. T.; Busse, C.; Michely, T. Dirac Cones and Minigaps for Graphene on Ir(111). *Phys. Rev. Lett.* **2009**, *102*, 056808.
21. Shikin, A. M.; Prudnikova, G. V.; Adamchuk, V. K.; Moresco, F.; Rieder, K.-H. Surface Intercalation of Gold Underneath a Graphite Monolayer on Ni(111) Studied by Angle-Resolved Photoemission and High-Resolution Electron-Energy-Loss Spectroscopy. *Phys. Rev. B* **2000**, *62*, 13202.
22. Varykhalov, A.; Sánchez-Barriga, J.; Shikin, A. M.; Biswas, C.; Vescovo, E.; Rybkin, A.; Marchenko, D.; Rader, O. Electronic and Magnetic Properties of Quasifreestanding Graphene on Ni. *Phys. Rev. Lett.* **2008**, *101*, 157601.
23. Haberer, D.; Vyalikh, D. V.; Taioli, S.; Dora, B.; Farjam, M.; Fink, J.; Marchenko, D.; Pichler, T.; Ziegler, K.; Simonucci, S.; *et al.* Tunable Band Gap in Hydrogenated Quasi-Free-Standing Graphene. *Nano Lett.* **2010**, *10*, 3360–3366.
24. Riedl, C.; Coletti, C.; Iwasaki, T.; Zakharov, A. A.; Starke, U. Quasi-Free-Standing Epitaxial Graphene on SiC Obtained by Hydrogen Intercalation. *Phys. Rev. Lett.* **2009**, *103*, 246804.
25. Balog, R.; Jorgensen, B.; Nilsson, L.; Andersen, M.; Rienks, E.; Bianchi, M.; Fanetti, M.; Laegsgaard, E.; Baraldi, A.; Lizzit, S.; *et al.* Bandgap Opening in Graphene Induced by Patterned Hydrogen Adsorption. *Nat. Mater.* **2010**, *9*, 315–319.
26. Usachov, D.; Dobrotvorskii, A. M.; Varykhalov, A.; Rader, O.; Gudat, W.; Shikin, A. M.; Adamchuk, V. K. Experimental and Theoretical Study of the Morphology of Commensurate and Incommensurate Graphene Layers on Ni Single-Crystal Surfaces. *Phys. Rev. B* **2008**, *78*, 085403.
27. Sutter, P. W.; Flege, J.-I.; Sutter, E. A. Epitaxial Graphene on Ruthenium. *Nat. Mater.* **2008**, *7*, 406–411.
28. Coraux, J.; N'Diaye, A. T.; Engler, M.; Busse, C.; Wall, D.; Buckanie, N.; zu Heringdorf, F.-J. M.; van Gastel, R.; Poelsema, B.; Michely, T. Growth of Graphene on Ir(111). *New J. Phys.* **2009**, *11*, 023006.
29. Grüneis, A.; Vyalikh, D. V. Tunable Hybridization between Electronic States of Graphene and a Metal Surface. *Phys. Rev. B* **2008**, *77*, 193401.
30. Kang, M. H.; Jung, S. C.; Park, J. W. Density Functional Study of the Au-Intercalated Graphene/Ni(111) Surface. *Phys. Rev. B* **2010**, *82*, 085409.
31. Braun, K.-F.; Rieder, K.-H. Ni(111) Surface State Observed with Scanning Tunneling Microscopy. *Phys. Rev. B* **2008**, *77*, 245429.
32. Dzemiantsova, L. V.; Karolak, M.; Lofink, F.; Kubetzka, A.; Sachs, B.; von Bergmann, K.; Hankemeier, S.; Wehling, T. O.; Frömter, R.; Oepen, H. P.; *et al.* Multiscale Magnetic Study of Ni(111) and Graphene on Ni(111). *Phys. Rev. B* **2011**, *84*, 205431.
33. Wallace, P. R. The Band Theory of Graphite. *Phys. Rev.* **1947**, *71*, 622–634.
34. Neto, A. H. C.; Guinea, F.; Peres, N. M. R.; Novoselov, K. S.; Geim, A. K. The Electronic Properties of Graphene. *Rev. Mod. Phys.* **2009**, *81*, 109.
35. Li, G.; Luican, A.; Andrei, E. Y. Scanning Tunneling Spectroscopy of Graphene on Graphite. *Phys. Rev. Lett.* **2009**, *102*, 176804.
36. Hornekær, L.; Šljivančanin, Z.; Xu, W.; Otero, R.; Rauls, E.; Stensgaard, I.; Lægsgaard, E.; Hammer, B.; Besenbacher, F. Metastable Structures and Recombination Pathways for Atomic Hydrogen on the Graphite (0001) Surface. *Phys. Rev. Lett.* **2006**, *96*, 156104.
37. Guisinger, N. P.; Rutter, G. M.; Crain, J. N.; First, P. N.; Stroscio, J. A. Exposure of Epitaxial Graphene on SiC(0001) to Atomic Hydrogen. *Nano Lett.* **2009**, *9*, 1462–1466.
38. Balog, R.; Jorgensen, B.; Wells, J.; Laegsgaard, E.; Hofmann, P.; Besenbacher, F.; Hornekaer, L. Atomic Hydrogen Adsorbate Structures on Graphene. *J. Am. Chem. Soc.* **2009**, *131*, 8744–8745.
39. Farjam, M.; Haberer, D.; Grüneis, A. Effect of Hydrogen Adsorption on the Quasiparticle Spectra of Graphene. *Phys. Rev. B* **2011**, *83*, 193411.
40. Ferro, Y.; Teillet-Billy, D.; Rougeau, N.; Sidis, V.; Morisset, S.; Allouche, A. Stability and Magnetism of Hydrogen Dimers on Graphene. *Phys. Rev. B* **2008**, *78*, 085417.
41. Sljivancanin, Z.; Rauls, E.; Hornekaer, L.; Xu, W.; Besenbacher, F.; Hammer, B. Extended Atomic Hydrogen Dimer Configurations on the Graphite(0001) Surface. *J. Chem. Phys.* **2009**, *131*, 084706.
42. Duplock, E. J.; Scheffler, M.; Lindan, P. J. D. Hallmark of Perfect Graphene. *Phys. Rev. Lett.* **2004**, *92*, 225502.
43. Yuan, S.; De Raedt, H.; Katsnelson, M. I. Modeling Electronic Structure and Transport Properties of Graphene with Resonant Scattering Centers. *Phys. Rev. B* **2010**, *82*, 115448.
44. Wong, S. L.; Huang, H.; Wang, Y.; Cao, L.; Qi, D.; Santoso, I.; Chen, W.; Wee, A. T. S. Quasi-Free-Standing Epitaxial Graphene on SiC (0001) by Fluorine Intercalation from a Molecular Source. *ACS Nano* **2011**, *5*, 7662–7668.
45. Ugeda, M. M.; Brihuega, I.; Guinea, F.; Gómez-Rodríguez, J. M. Missing Atom as a Source of Carbon Magnetism. *Phys. Rev. Lett.* **2010**, *104*, 096804.
46. Haberer, D.; Petaccia, L.; Farjam, M.; Taioli, S.; Jafari, S. A.; Nefedov, A.; Zhang, W.; Calliari, L.; Scarduelli, G.; Dora, B.; *et al.* Direct Observation of a Dispersionless Impurity Band in Hydrogenated Graphene. *Phys. Rev. B* **2011**, *83*, 165433.
47. Grüneis, A.; Attaccalite, C.; Rubio, A.; Vyalikh, D. V.; Molodtsov, S. L.; Fink, J.; Follath, R.; Eberhardt, W.; Büchner, B.; Pichler, T. Angle-Resolved Photoemission Study of the Graphite Intercalation Compound KC_8: A Key to Graphene. *Phys. Rev. B* **2009**, *80*, 075431.
48. Bianchi, M.; Rienks, E. D. L.; Lizzit, S.; Baraldi, A.; Balog, R.; Hornekær, L.; Hofmann, P. Electron−Phonon Coupling in Potassium-Doped Graphene: Angle-Resolved Photoemission Spectroscopy. *Phys. Rev. B* **2010**, *81*, 041403.
49. Bostwick, A.; Speck, F.; Seyller, T.; Horn, K.; Polini, M.; Asgari, R.; MacDonald, A. H.; Rotenberg, E. Observation of Plasmarons in Quasi-Freestanding Doped Graphene. *Science* **2010**, *328*, 999–1002.
50. Palacios, J. J.; Fernández-Rossier, J.; Brey, L. Vacancy-Induced Magnetism in Graphene and Graphene Ribbons. *Phys. Rev. B* **2008**, *77*, 195428.
51. Grüneis, A.; Kummer, K.; Vyalikh, D. V. Dynamics of Graphene Growth on a Metal Surface: A Time-Dependent Photoemission Study. *New J. Phys.* **2009**, *11*, 073050.
52. Hornekær, L.; Rauls, E.; Xu, W.; Šljivančanin, V.; Otero, R.; Stensgaard, I.; Lægsgaard, E.; Hammer, B.; Besenbacher, F. Clustering of Chemisorbed H(D) Atoms on the Graphite (0001) Surface Due to Preferential Sticking. *Phys. Rev. Lett.* **2006**, *97*, 186102.
53. Haberer, D.; Giusca, C. E.; Wang, Y.; Sachdev, H.; Fedorov, A. V.; Farjam, M.; Jafari, S. A.; Vyalikh, D. V.; Usachov, D.; Liu, X.; *et al.* Evidence for a New Two-Dimensional C4H-Type Polymer Based on Hydrogenated Graphene. *Adv. Mater.* **2011**, *23*, 4497–4503.
54. Horcas, I.; Fernández, R.; Rodríguez, J. M. G.; Colchero, J.; Herrero, J. G.; Baro, A. M. WSXM: A Software for Scanning Probe Microscopy and a Tool for Nanotechnology. *Rev. Sci. Instrum.* **2007**, *78*, 013705.
55. Petaccia, L.; Vilmercati, P.; Gorovikov, S.; Barnaba, M.; Bianco, A.; Cocco, D.; Masciovecchio, C.; Goldoni, A. BaD ElPh: A 4 m Normal-Incidence Monochromator Beamline at Elettra. *Nucl. Instrum. Methods Phys. Res., Sect. A* **2009**, *606*, 780–784.
56. Aradi, B.; Hourahine, B.; Frauenheim, T. DFTB+, a Sparse Matrix-Based Implementation of the DFTB Method. *J. Phys. Chem. A* **2007**, *111*, 5678–5684.

57. Elstner, M.; Porezag, D.; Jungnickel, G.; Elsner, J.; Haugk, M.; Frauenheim, T.; Suhai, S.; Seifert, G. Self-Consistent-Charge Density-Functional Tight-Binding Method for Simulations of Complex Materials Properties. *Phys. Rev. B* **1998**, *58*, 7260–7268.
58. Humphrey, W.; Dalke, A.; Schulten, K. VMD: Visual Molecular Dynamics. *J. Mol. Graphics* **1996**, *14*, 33–38.